NASA

Technical Memorandum 79577

OSO-8 X-Ray Spectra of Clusters of Galaxies. II. Discussion

Barham W. Smith, R. F. Mushotzky
and P. J. Serlemitsos

JULY 1978

National Aeronautics and
Space Administration

Goddard Space Flight Center
Greenbelt, Maryland 20771

OSO-8 X-RAY SPECTRA OF CLUSTERS OF GALAXIES.
II. DISCUSSION

Barham W. Smith[*], R. F. Mushotzky[**], and P. J. Serlemitsos

Laboratory for High Energy Astrophysics
NASA/Goddard Space Flight Center
Greenbelt, Maryland 20771

ABSTRACT

The Goddard Space Flight Center 2 to 20 keV OSO-8 data on X-ray clusters is examined for information which will restrict models for hot intracluster gas structures. Our starting point is the correlations between X-ray spectral parameters and optical cluster properties which we presented in a previous paper (Mushotzky et al.; Paper I).

From the correlation between X-ray temperature and velocity dispersion, we conclude that the X-ray core radius should be less than the galaxy core radius, if we assume the gas is isothermal. Thus fits of X-ray profiles of clusters to isothermal spheres yield a core radius approximately equal to the density cutoff radius rather than the true core radius. If we instead assume a generalized polytropic structure, from the same correlation one may conclude that the gas is more nearly isothermal than adiabatic within a few core radii of the center. Therefore we require thermal conduction, radiative cooling, or both in cluster atmospheres. In both of these interpretations, the Coma cluster and possibly Abell 2319A are quite discrepant.

From the correlation between bremsstrahlung emission integral and temperature, we conclude that hotter clusters contain a larger fraction of

---

[*] Also Dept. of Physics and Astronomy, Univ. of Maryland
[**] NAS/NRC Research Associate

their virial mass in the form of gas emitting in the 2 to 20 keV band. This conclusion depends on the adoption of the X-ray size measurements of clusters from UHURU data by Kellogg and Murray. We find that the "central concentration factor" for the emission cannot vary with temperature steeply enough to account for the correlation.

We closely examine relations among the various measures of galaxy density and optical cluster morphology. There is evidence for real correlations between optical _central_ cluster properties and X-ray properties which are not "artifacts" of underlying richness correlations as suggested by Jones and Forman.

We also predict a population of cool, dim X-ray clusters which has not been observed.

From consideration of the errors in published atomic physics data and spectrum calculations, we conclude that the iron abundance determinations recently quoted for intracluster gas are uncertain by 50 to greater than 100 percent from this nonstatistical cause alone.

Subject headings: galaxies: clusters of--galaxies: intergalactic medium--
                   X-ray: spectra

I. INTRODUCTION

In the previous paper (Mushotzky et al. 1978; hereafter Paper
I) we presented X-ray results for spatially integrated spectra of twenty
clusters of galaxies observed by the GSFC Cosmic X-ray Spectroscopy
experiment aboard the OSO-8 satellite. For these clusters we found
best fitting temperatures, bremsstrahlung emission integrals, and iron
abundances (derived from measurements of iron emission line features
at 6.7 to 6.9 keV). Because our sample of these measured quantities
is the largest to date, we were able to investigate new correlations
between physically interesting X-ray and optically determined cluster
parameters. In turn, the correlations we found, combined with the
result that all the clusters could have the same iron abundance, led
us to confirm that the X-ray emission from clusters in the 2 to 20
keV band is primarily thermal radiation from hot intracluster gas,
with perhaps half this gas having come from inside galaxies. In this
paper we present no further data, but sketch a broader view of the
significance of our results against the background of other work.

Our goal is an observational description of X-ray clusters of
galaxies. Correlations involving the physical quantities that can
only be determined by spectroscopic measurements contribute much to
our understanding. In the next few sections we examine certain con-
clusions that can be drawn from the correlations in Paper I. We find
from the temperature-velocity dispersion correlation that the X-ray
core radius should be less than the galaxy core radius, or, alternatively,
that the polytropic index is about 1.1 for most of our clusters. Analysis

of the temperature-emission integral correlation yields evidence that more massive clusters accumulate a larger fraction of their mass as intracluster gas. We also reexamine galaxy densities and optical morphology, as they correlate with X-ray properties, for clues as to how mass injection by galaxies affects the density structure of the gas. Then, we discuss the predictions that can be made from our correlations and the impact of all these results on models for intracluster atmospheres. Finally, we devote a section to a critical appraisal of the physical arguments used to derive iron abundances from observed equivalent widths of iron line features in X-ray spectra, and we estimate the associated uncertainties in abundances derived in this way. Our conclusions are collected into § IX.

It is necessary here to repeat that this discussion assumes that the identifications of X-ray sources with the clusters we include are correct. Doubt has recently been thrown on the identification of SC1251-28 as an X-ray source (Cooke 1978). In this paper we continue our policy in Paper I of treating these twenty identifications as real.

II. THE VELOCITY DISPERSION VS. TEMPERATURE RELATION

a)   The Observed Relation

If intracluster gas is bound in the gravitational potential of a cluster of galaxies which are themselves gravitationally bound, the virial theorem can be applied to relate the velocity dispersion of the galaxies to the cluster mass, and the cluster mass to the X-ray temperature. There is evidence that the gas of galaxies in a cluster is approximately isothermal, at least in the central regions, in which

case the central velocity dispersion Δv_c measures the core mass M_c

(see Paper I). If some heat transport process also enforces isothermality

in the gas, the temperature T should be proportional to Δv^2. If T is

interpreted as an <u>average</u> X-ray temperature in the emitting region, then

$T \propto \Delta v^2$ to first order even without isothermality. In Paper I we found

the best fitting slope of a function $T = A \Delta v_c^{\alpha}$ was $\alpha = 1.6 \pm .3$, but α

was pushed below 2 largely due to the influence of the Coma point,

which is clearly off the trend of the remaining data. We suggested

a relation leaving out clusters of Rood-Sastry (1971) type cD and B,

which leaves the other clusters along a line $\alpha \approx 2.0$, but in fact only

Coma and A2319A need be omitted from the data set to obtain $\alpha \approx 2.0$.

It may or may not be significant that these two clusters are the highest

temperature X-ray clusters for which T and Δv have both been measured.

Coma is the best studied cluster optically, and it seems impossible

that the central velocity dispersion is significantly higher than 1050

km s^{-1}. The velocity dispersion of Abell 2319 is more doubtful. Although

Faber and Dressler (1976) show some evidence that A2319A and B are

separate clusters, the X-ray position (Grindlay <u>et al.</u> 1977) does not

exclude the possibility that the X-ray emission is associated with

some combination of A and B. If Δv for the combination is adopted,

A2319 falls on the projected trend of the Δv vs. T relation fixed by

lower temperature clusters.

A relation between T and Δv very similar to ours was given by

Mitchell, Ives, and Culhane (1977). Some of their temperature determin-

ations are significantly lower than ours (notably for Coma and Centaurus),

for reasons not clear to us. However, even with their lower temperature

for Coma, Mitchell et al. found that it had a low velocity dispersion

for its temperature compared to the other clusters in their sample.

b)   The Extent of the Gas

Since we have good reason to believe T is roughly proportional

to Δv^2, we seek an explanation for the value of the proportionality

constant. Cavaliere and Fusco-Femiano (1976) have shown that the extent

of the gas relative to the galaxies is dependent on the ratio of specific

kinetic energies of galaxies and gas. If m is the average particle

mass (fully ionized gas with 10% He), this ratio is given by

$$\varepsilon \equiv \frac{m\Delta v^2}{kT} \approx 6.3 \left(\frac{\Delta v}{1000 \text{ km s}^{-1}}\right)^2 \left(\frac{1 \text{ keV}}{kT}\right) , \qquad (1)$$

The cluster used by Cavaliere and Fusco-Femiano as an example of the

value of ε is Coma, for which our data give $\varepsilon \approx 0.6$ in rough agreement

with their value. This uses the mean rather than the central velocity

dispersion. We have seen that Coma lies well below the trend in the

Δv vs. T relation, and we suggest it may not be a good example. As

illustration we calculate ε and $\varepsilon_c = (1.17)^2 \varepsilon$ individually for each

cluster in Paper I, Fig. 5, using the most probable value of kT and Δv

as given in Tables 2 and 3 of that paper. The results, given in Table

1, indicate that $\varepsilon \gtrsim 1.1$ and $\varepsilon_c \gtrsim 1.5$ for most clusters.

When we used the word extent above, we meant the core radius

of the spherical distribution of galaxies or gas. The core radius is the

parameter a in the standard approximation to an isothermal sphere, n(r) =

$n_0 (1 + r^2/a^2)^{-3/2}$; namely a_g for the galaxies and a_x for the X-ray

emitting gas.   Since the gas density as a function of radius in the

outer regions of an intracluster atmosphere depends on the total mass of gas, the core radius alone does not determine how far from the center gas may be found. The ratio ε should be a direct comparison of the core radii of galaxy and gas distributions if both are isothermal. Values of $\varepsilon > 1$ imply that the galaxies are more extended than the gas, in terms of core radii. This extent refers to the density distribution, so the surface brightness, proportional to n^2 through the emission measure, will be more sharply peaked, i.e. have somewhat smaller core radius. This interpretation of the Δv vs. T relation makes it easier to understand how intracluster gas could be largely processed gas, ejected from cluster member galaxies and collected near the cluster center; if the galaxies were less extended in terms of core radius than the gas as has been suggested from previous analyses of X-ray emission profiles (Lea 1975, Cavaliere and Fusco-Femiano 1976), some heating mechanism for this gas would be required in addition to conversion of kinetic energy of galaxy motions into thermal energy. Primordial gas falling into the cluster as a continuation of the cluster formation process (Gunn and Gott 1972) would also be expected to have a smaller core radius than the galaxy core radius, since the gas relaxes much faster than the cloud of galaxies. Thus for the combination of roughly half processed and half primordial gas implied by our iron abundance measurements, we expect $\varepsilon > 1$. And as we mentioned in Paper I, the best fit to the Δv vs. kT relation corresponds to the case where the gas is in equilibrium at approximately its gravitational temperature. Incidentally, it is difficult to explain the low value of ε for Coma

by postulating some nonthermal heating of its gas, because radio
observations indicate there have been no major outbursts from active
galaxies in Coma for about 10^9 yrs (Willson 1970). However, Lea and
Holman (1978) show that significant Coulomb heating of the gas can
occur if the magnetic field is sufficiently low.

If the distribution of either gas or galaxies is not strictly
isothermal, then the parameter ϵ has a somewhat more complex interpretation.
Yet the King (1972) model usually adopted for the galaxy distribution
is nearly isothermal near the core, and our observations of the strong
X-ray cluster Perseus indicate that its spectrum is not far from isothermal
(Smith et al. 1978).

In any case, values of $\epsilon > 1$ are interesting since fits to X-ray
profiles of clusters using this standard approximation to isothermal
spheres in the past (e.g. Kellogg and Murray 1974) have led to X-ray
core radii a_x greater than a_g. This contradiction is merely the re-
flection of the fact that the overall gas distribution is not an isothermal
sphere with infinite extent. If the density (and hence surface brightness)
falls off rapidly beyond some cutoff radius r_{co}, a fit to the surface
brightness using an isothermal sphere will give an apparent $a_x \approx r_{co}$
and not the true a_x which is related to ϵ. Interestingly, the evolutionary
models of Perrenod (1978a) for intracluster gas would also give apparent
values of a_x (in the ½ to 2 keV band, however) larger than a_g, because
his gas distributions have sharp density cutoffs at $r_{co} > a_g$. We discuss
these and other models in more detail in §VII.

c) The Polytropic Index of the Gas

Should one wish to relax the requirement that the gas be isothermal, the next simplest equation of state to work with is a polytropic one ($P \propto n^\gamma$ where γ is the polytropic index). In spherically symmetric, hydrostatic models for cluster atmospheres using this equation, the temperature varies with radius for any $1 < \gamma \leq 5/3$. For Paper I we performed isothermal fits to our spectral data, but we now wish to consider models in which the X-ray continuum is the sum or integral over contributions from shells at different temperatures. However, without fitting trial spectra representing these more complicated continua (a tedious and statistically unjustifiable procedure), we can learn something about the characteristics of acceptable spectra and hence about acceptable gas distributions, although this knowledge will be of a rough nature. The technique rests upon the fact that the <u>central</u> temperature of hydrostatic models is still proportional to Δv_c^2. We now review enough results on polytropic, hydrostatic, spherically symmetric gas distributions in cluster potentials to enable us to derive the equation relating our measured X-ray temperature to Δv_c and γ.

Defining x as the radius in units of a_g, the temperature structure is (Lea 1977)

$$kT(x) = \left[\phi(x) - \phi(x_{out}) \right] m \frac{\gamma - 1}{\gamma}, \qquad (2)$$

where ϕ is the absolute value of the gravitational potential. The "outer radius" x_{out} is determined from

$$kT_\infty = -\phi(x_{out}) m \frac{\gamma - 1}{\gamma}, \qquad (3)$$

where the "temperature" T_∞ indicates the degree to which gas is bound to the cluster at infinite distance. Thus x_{out} is the ultimate extent of the gas cloud and the distance at which an exponential drop of the radial density law is found. We restrict T_∞ to negative values for this discussion, implying zero gas pressure at infinity and binding all gas to the cluster. However, this choice excludes cluster gas structures connecting smoothly to a universal hot intergalactic medium (e.g. Field and Perrenod 1977) or to supercluster gas (Perrenod 1978b). The gravitational potential in equations (2) and (3) may be expressed with the use of the analytic approximation given by King (1972) for the mass distribution, yielding

$$\phi(x) = \frac{3GM_c}{a_g} \frac{1}{x} \ln\left[x + (1 + x^2)^{1/2}\right] \equiv \frac{3GM_c}{a_g} g(x), \tag{4}$$

where M_c is the core virial mass and we define the function $g(x)$ for future convenience.

In cases where gas at more than one temperature contributes to X-ray emission in the 2-20 keV band, the temperature we have measured for each cluster in our sample in Paper I is a particular weighted average temperature. This observed temperature parameter, which we henceforth call $\bar{T}$, characterizes the best fit to the data of isothermal trial spectra in the least squares sense. To relate the polytropic index γ to $\bar{T}$, we note that $g(x=0) = 1$, so that from (2) and (4) the central temperature T_c of our polytropic gas distribution is given by

$$T_c \equiv T(x=0) = \frac{3GM_c}{a_g} \frac{m}{k} \frac{\gamma - 1}{\gamma} \left[1 - g(x_{out}) \right] . \qquad (5)$$

In order to find how $\bar{T}$ is related to γ, T_c, and x_{out} we performed calculations of the expected shapes of continuum spectra that would result from polytropic gas distributions and treated them as synthetic data sets. We fitted them to isothermal trial spectra within the same energy band (2 to 20 keV) as our real cluster data, using the same least squares goodness-of-fit criterion. The results of an extensive grid of polytropic models and isothermal fits can be expressed as a table of values of the ratio $\bar{T}/T_c \equiv \tau(\gamma, T_c, x_{out})$. Values of τ are given in Table 2. It is important to keep in mind that these values are dependent on the energy band and goodness-of-fit test. Making use of the virial theorem for the core, $GM_c/a_g = 3(\Delta v_c)^2$, we have numerically

$$k\bar{T}(keV) \approx 56 \left(\frac{\Delta v_c}{1000 \text{ km s}^{-1}} \right)^2 \frac{\gamma_{eff}-1}{\gamma_{eff}} \tau(\gamma_{eff}, T_c, x_{out}) \left[1-g(x_{out}) \right] . \qquad (6)$$

Given $\bar{T}$ and Δv_c for a cluster, one may find what combination of γ_{eff}, T_c, and x_{out} are compatible with the data, by iteratively seeking to satisfy equation (6). With an assumption about the unknown value of x_{out}, one can obtain limits on γ_{eff}. We introduce the notation γ_{eff}, the effective polytropic index, to indicate that by this method we are estimating the logarithmic slope of whatever equation of state $P = P(n)$ is followed by intracluster gas, as long as the gas structure meets conditions of spherical symmetry and approximate hydrostasis. We discuss this further in §VII. The value of x_{out} can in principle

be determined from spatially resolved observations of clusters, but to date there has not been sufficient knowledge of physical conditions far from the cluster center to allow it to be determined convincingly. Lea (1977) suggests that clusters are observed optically out to $x \gtrsim 40$, implying that one might choose this value, but we have seen that the core radius for isothermal distributions of gas is probably less than that of galaxies, and x_{out} for the gas is nowhere required to be the same as the outer radius of the galaxy distribution. Fortunately, it turns out that when γ_{eff} is determined for some cluster from (6), its value is not very dependent on the assumed value of x_{out}, as long as $x_{out} \gtrsim 10$.

In Figure 1 we repeat the Δv_c and $\overline{T}$ data from Paper I overlaid with lines of constant γ_{eff} (variable T_c) and constant T_c (variable γ_{eff}) from the results of our synthetic data fits. We emphasize that this presentation assumes $T_c \propto \Delta v_c^2$. Estimates of the best value of γ_{eff} can be read directly from Figure 1 for each cluster. The arithmetic mean of best values for all clusters in the figure is $\gamma_{eff} = 1.08$. The 90% confidence limits on $\overline{T}$ restrict the values of γ_{eff} to values less than about 1.1 for most clusters, independent of T_c or x_{out} within reasonable bounds. Coma again stands alone as having a higher than average γ_{eff}, and due to the crossing of lines of constant γ_{eff} near its position in Figure 1, its effective polytropic index is relatively indeterminate, $1.15 < \gamma_{Coma} < 5/3$[1].

---

[1]Values of γ_{eff} greater than 5/3 or less than 1 are not unphysical, strictly speaking, if thermal instabilities or nonuniform heating occur

in cluster atmospheres. We ignore the complications of nonequilibrium phenomena and inhomogeneous conditions when we approximate arbitrary equations of state by polytropic power laws.

Abell 2319A lies in a region which is forbidden to equilibrium models, but $\gamma \simeq 5/3$ is just allowed by the error limits.

Malina et al. (1978) have derived limits on γ_{eff} for Coma and Perseus based on available X-ray data at their writing, including spatially resolved soft X-ray measurements. They found $1.18 < \gamma_{eff} < 1.5$ for Coma and $1 < \gamma_{eff} < 1.15$ for Perseus, which agree quite well with our values.

III. THE GALAXY DENSITY VS. TEMPERATURE RELATION

In a similar way we can analyze the correlation we found in Paper I between $\overline{T}$ and the central galaxy density of Bahcall (1977), $\overline{N}_0$. A calibration between $\overline{N}_0$ and Δv can be found from Figure 2, where these quantities are plotted for clusters having both measurements. Evidence that $\overline{N}_0$ can also be used as a measure of virial mass, a theoretically attractive concept, is seen in the appropriateness of the fit

$$\overline{N}_0 \text{ (galaxies per } \tfrac{\pi}{4} \text{ Mpc}^2) \simeq (22 \pm 2) \; (\frac{v}{1000 \text{ km s}^{-1}})^2. \qquad (7)$$

Using this calibration, the $\overline{N}_0$ vs. $\overline{T}$ relation, Figure 7 of Paper I, can be analyzed to yield either ε or γ_{eff} for each cluster. The numerical relation involving γ_{eff} is

$$k\overline{T}(keV) \simeq 3.7 \; \overline{N}_0 \; \frac{\gamma_{eff} - 1}{\gamma_{eff}} \; \tau \; (\gamma_{eff}, \; T_c, \; x_{out}) \left[1 - g(x_{out}) \right]. \qquad (8)$$

The numbers for most clusters are not very different from what one would derive from the Δv vs. $\bar{T}$ relation, but some clusters depart from the trend of Figure 2 and thus yield different ϵ and γ_{eff} when $\bar{N}_0$ vs. $\bar{T}$ is used. The results for Coma are significantly different, with $\gamma_{eff} \approx 1.1$ from $\bar{N}_0$, substantially lower than γ_{eff} from Δv_c. In contrast $\gamma_{eff} \approx 1.2$ for A2147 from $\bar{N}_0$ is higher than its value from Δv. These departures in Figure 2 may be explicable as some combination of optical measurement errors in the quantities $\bar{N}_0$ and Δv. Aside from these anomalies, the similarity of the best fits to Δv_c vs. $\bar{T}$ and $\bar{N}_0$ vs. $\bar{T}$ encourages the attractive view that most clusters fall on one joint sequence of temperature and virial mass. Measurements of $\bar{N}_0$ should be inherently less sensitive than those of Δv to errors from inclusion of stray objects or exclusion of true cluster members. We need not emphasize that measurements of more clusters are needed.

IV. THE EMISSION INTEGRAL VS. TEMPERATURE RELATION

The bremsstrahlung luminosity is proportional to the emission integral (hereafter EI), which is the average of density squared over the emission volume, multiplied by that volume, and is denoted $<n^2>V$. From observations with a field of view larger than $V^{1/3}$, one cannot reduce EI to its component factors n and V. However, by using all available clues to the sizes of the volumes in various clusters, we might hope to make some progress in factoring EI. It is important that we try, because the mass of gas cannot be derived from EI without V and $<n>$ (not $<n^2>$). Thus we need some idea of how n depends on radius from a cluster center.

The EI vs. $\bar{T}$ relation found in Paper I is particularly important, because while $\bar{T}$ is believed sensitive to the depth of the potential, EI is sensitive to the amount of gas (if we know the density distribution). Thus a correlation between them implies some connection in clusters between the mass of gas and the mass of galaxies. The value of such a connection is determined by the number of assumptions one must make to formulate a useful interpretation. As briefly explained in Paper I, if one relates the mass of intracluster gas to the total virial mass of the cluster by $M_{gas} = \mu M_{vir}$ (where we must restrict M_{gas} to represent only that part of the gas which emits X-rays in the 2 to 20 keV band), then

$$EI \propto \frac{\mu^2 f \ \bar{T}^2 \ a_g^2}{V} , \qquad (9)$$

where $f \equiv <n^2>/<n>^2 > 1$ is an overall central concentration factor for the gas. The result from Paper I can be expressed as $EI \propto \bar{T}^\beta$, $1.6 \lesssim \beta \lesssim 5.1$, although scatter in the correlation prevents an acceptable fit to a single power law. This correlation is probably not due to selection effects since only clusters with both low EI and low $\bar{T}$ are strongly selected against. The trend can be seen solely from the apparently excluded regions at high EI/low $\bar{T}$ and low EI/high $\bar{T}$. We can eliminate the core radius a_g from (9) right away. Plotting Bahcall's (1975) optical measurements of a_g for different clusters in our temperature sample against $\bar{T}$ shows no indication that a_g is related to $\bar{T}$; in fact, she finds $a_g \approx .25$ Mpc for all clusters with a probable error of $\pm 15\%$, an error range smaller than the uncertainties in the $\bar{T}$ and EI data. Therefore

$$\frac{\mu^2 f}{V} \quad \propto \quad \overline{T}^{\beta-2} \tag{10}$$

with good confidence. To make further progress we must know how μ, f, or V depend on temperature.

The sizes of regions contributing to the 2 to 6 keV flux have been measured by Kellogg and Murray (1974) and all the clusters in their list were included in Paper I. Their sizes are given as apparent X-ray core radii a_x for the standard approximation to hydrostatic isothermal sphere models with infinite extent. Hereafter we call their measured parameter R_x to emphasize that it is an observational quantity and may not be the true a_x which is related to the density distribution in the isothermal region of a realistic model. We treat R_x as some characteristic radius and trust that values of R_x are indicative of relative size between clusters. In Figure 3 we show R_x vs. $\overline{T}$ including the upper limits in Kellogg and Murray. The four clusters known by their constellations and having the highest X-ray flux lie on a straight line, whose slope is rather dependent on the Virgo point. This line suggests $R_x \propto \overline{T}^\eta$ with $\eta \approx 5/4$. When Abell 2256 and 262 are included in the fit, one obtains instead $1.5 \lesssim \eta \lesssim 1.8$, but these two clusters have considerably weaker flux, and we feel that their sizes are perhaps less certain than is indicated by the error limits given in Kellogg and Murray. All in all, $1.2 \lesssim \eta \lesssim 1.8$ is probably a fair representation of the slope of the R_x vs. $\overline{T}$ relation.

If we adopt this apparent temperature dependence of R_x from UHURU data (Case A), we have $\mu^2 f \propto \overline{T}^{\beta-2+3\eta}$. To subdivide further we consider

two simple cases: (Case 1) μ is independent of $\bar{T}$, which fixes a range
of logarithmic slopes for f(T); (Case 2) f is independent of $\bar{T}$, which
fixes the slope of μ(T). In view of the importance of the Virgo point
in tying down the low end of the R_X vs. $\bar{T}$ correlation and the possibility
that the gas in Virgo is associated with a single galaxy and has a
size not comparable with the other clusters, it is also worthwhile
to consider the consequences of removing this data point. There is
then no obvious correlation between R_X and $\bar{T}$ (Case B), and we have
$\mu^2 f \propto \bar{T}^{\beta-2}$ from which we can again derive the plausible ranges of
slopes for f(T) or μ(T) in Cases 1 and 2 above. In Table 3 we show
limits to these slopes. Values of δ and ζ for the four cases have
little overlap in spite of their wide range. However, for V independent
of $\bar{T}$, δ or ζ may be zero, in which event μ and f might both be independent
of $\bar{T}$; this null temperature dependence reflects the fact that β may
be 2 in equation (10).

In trying to eliminate some of these possibilities, we can say
nothing a priori about the temperature dependence of μ. However, in
Case 1A the central concentration factor f contains a strong temperature
dependence. We might ask whether f can vary over the required range
within the roughly order of magnitude temperature variation of our
clusters. To be specific, between $2 < \bar{T} < 13$ keV, a factor of six
in $\bar{T}$, we would require f to vary by 6^δ, $3.2 < \delta < 8.5$, or by a factor
between 310 and 4.1×10^6. Since polytropic models with $\gamma \approx 1.1$ are
probably good approximations to the X-ray spectral data in Paper I,
we have calculated values of f for a range of γ and x_{out}, and we present

the results in Figure 4. The density integrals have been cut off at a radius x_{band} so that f values will be useful for interpretation of our EI data. Beyond x_{band}, the temperature is assumed to fall below that which contributes bremsstrahlung emission to some given energy band. In the 2-20 keV band the lowest temperature that can be detected in clusters is about 1 keV. Figure 4 can be used for other bands since polytropic models may be normalized arbitrarily. There is a discontinuity between polytropic models, all of which have the same T(x) fall-off with radius for the same x_{out}, and isothermal models which have no temperature fall-off. Realistic isothermal models have f not very different from our $\gamma = 1.1$ calculations. This causes some difficulty in the interpretation of f for low values of γ, which can only be resolved by considering more physically realistic models. For the present discussion, it is sufficient to consider Figure 4. Choosing T_c for some model from Figure 1 determines $T(x_{band})/T_c$, if $T(x_{band})$ is always 1 keV. This determines a range of x_{out} and x_{band} from Figure 4a, and then a range of f is obtained from Figure 4b. We have calculated f for a reasonable range of x_{out} (from the Abell radius to $x_{out} = 1000$) and x_{band} (a range decided on after numerous integrations of models giving $\overline{T}$ agreeing with the Paper I data). Results for a wider range of x_{band} can be deduced from trends in Figure 4. From this procedure we conclude that a dependence of f as steep as $\overline{T}^{8.5}$ is impossible, because f cannot vary that widely in any polytropic model. Even a dependence $f \propto \overline{T}^{3.2}$ is difficult to attain if most clusters have $\gamma \approx 1.1$. In short, Case IA is improbable for any reasonable variation

of γ and x_{out} from cluster to cluster.

The case with the fewest objections is Case 2A, since adoption of the UHURU size measurements (keeping in mind the importance of Virgo) eliminates Case B. Case 2A implies that hotter clusters have a larger fraction of their virial mass in the form of intergalactic gas emitting in the 2 to 20 keV band. The true temperature dependences of V, f, and μ may lie between the pure cases we have defined above, for example if all three have some dependence, but we suggest that some increase in μ with increasing $\bar{T}$ is required.

The only set of data with which to compare this result is discussed by Mitchell, Ives, and Culhane (1977). They consider the effect of a restricted energy band on the interpretation of their observed dependence of L_X on $\bar{T}$, but they ignore the central concentration factor f. They derive a relation $M_{gas} \propto \bar{T}^5$ for Case A and $M_{gas} \propto \bar{T}^2$ for Case B, which are consistent with our results, if reasonable assumptions about f are made. The observational relation on which these M_{gas} relations are based is $L_X \propto \bar{T}^{5.5}$ or roughly $EI \propto \bar{T}^5$, which lies just within the upper end of our range for β. When they plot R_X from Kellogg and Murray (1974) against their X-ray temperatures, they obtain $R_X \propto \bar{T}^2$ which is slightly too steep to be consistent with our results.

V. CORRELATIONS INVOLVING GALAXY DENSITIES

In Paper I we compared Abell's (1958) richness class R with the central galaxy density $\bar{N}_0$ of Bahcall (1977), and we found that $\bar{N}_0$ correlated better with $\bar{T}$ and EI than R did. These two indicators of galaxy density have now been joined by a third, the density $<\rho>$ calculated

by van den Bergh and deRoux (1978) on the basis of R and the cluster radii found by Leir and van den Bergh (1977). Moreover, $\overline{N}_0$, R, and $<\rho>$ may be related to the morphological types defined by Rood and Sastry (1971; hereafter RS) and by Bautz and Morgan (1970; hereafter BM). In this section we compare all these indicators of galaxy density and try to decide which are the most important for determining X-ray properties of clusters.

First, in Figure 5 we explicitly compare $\overline{N}_0$ and R for the cluster list given by Bahcall (1977), a comparison referred to in Paper I. The scatter is large, but similar to the scatter in the correlations of Paper I that involved $\overline{N}_0$. In Table 4 we begin to collect a set of quantitative measures of scatter, namely mean values and sample standard deviations (S.D.) for $\overline{N}_0$ and $<\rho>$ among various samples. The S.D. of $\overline{N}_0$ among R = 2 clusters (the most numerous richness class among known X-ray clusters) and kT > 6 keV clusters is similar. The latter S.D. is larger only because of the influence of Abell 2147 ($kT \approx 7$ keV, $\overline{N}_0$ = 12), which is peculiar on other grounds as seen in Figure 2. Returning to Figure 5, we see that $\overline{N}_0$ and R are weakly correlated, but indeed seem to be measuring different aspects of galaxy density, as suggested in Paper I. We have calculated van den Bergh and deRoux's new quantity $<\rho>$ for the known X-ray clusters in Bahcall's list. In contrast to the previous comparison, the probability of any correlation between $<\rho>$ and $\overline{N}_0$ is very small, although $<\rho>$ should be a more sophisticated indicator of galaxy density than plain richness class. This absence of correlation can also be seen in Table 4, where the average and S.D.

of $\overline{N}_0$ for two $<\rho>$ samples show that $<\rho>$ fails to distinguish high and
low $\overline{N}_0$, with scatter similar to or larger than in the $\overline{N}_0$ vs. R comparison.
Incidentally, $<\rho>$ correlates equally poorly with $\overline{T}$ or EI for our sample
of X-ray clusters. Perhaps the method used to determine cluster radii
by Leir and van den Bergh is too ill-suited for nearby clusters, such
as most known X-ray clusters.

Three weak correlations between galaxy densities and optical
morphological types have recently been suggested, namely between $\overline{N}_0$
and RS type (suggested but undocumented in Bahcall 1977), between R
and BM type (Leir and van den Bergh 1977), and between $<\rho>$ and BM type
(van den Bergh and deRoux 1978). We have given the RS type associated
with each point in Figure 5, so that the strength of the first of these
correlations can be examined. More centrally concentrated optical
appearance does occur more frequently at higher $\overline{N}_0$, but the scatter
in $\overline{N}_0$ among cD and C type clusters (see Table 4) is again large. The
R vs. BM type correlation is exhibited by Leir and van den Bergh and
amounts to a small excess of BM type I clusters in richer classes.
The $<\rho>$ vs. BM type relation appears stronger in the table of van den Bergh
and deRoux, but it is only visible in the mean values of $<\rho>$ for different
BM types, since the scatter of $<\rho>$ within BM types presented in Table
4 is the largest relative to the mean in the entire table. The redshift
range considered here, z > .1, is just beyond the redshift of the most
distant confirmed X-ray clusters and seems to have been chosen because
it is the range in which the cluster radius measurements of Leir and
van den Bergh should have the greatest reliability. However, we reluctantly

conclude that $<\rho>$ is not yet a useful quantity for X-ray work.

For the present purpose, we are left with $\overline{N}_0$ and R, as well as morphological type which seems to have some correlation with $\overline{N}_0$. But we believe that the scatter in the $\overline{N}_0$ vs. kT, $\overline{N}_0$ vs. EI, and $\overline{N}_0$ vs. R correlations is indicative of a situation in which several factors are participating or in which clusters evolve at different rates so that we see them in different stages. Let us keep these possibilities in mind in what follows. Of the morphological types, it does not seem to matter much whether RS or BM is used, since the correlation between them is fairly good among clusters which have been classified under both systems. Since RS type seems correlated with $\overline{N}_0$ to some extent, we concentrate on actual galaxy densities. We have discussed how $\overline{N}_0$ relates to X-ray data rather completely in Paper I, so we now consider richness.

Richness has often been suggested as an important parameter for determining the X-ray luminosity of clusters of galaxies. Most recently Jones and Forman (1978) and McHardy (1977) have found that L_x increases systematically with Abell richness class. Although Jones and Forman found no significant difference between the luminosities of R=0 and R=1 clusters, they did find that R=2 clusters were somewhat more luminous than the poorer classes. McHardy shows a clear progression of L_x through R=0, 1 and 2. Perhaps Jones and Forman did not distinguish R=0 and 1 because the R=0 cluster luminosities were overestimated relative to R=1 clusters. A comparison of the values of L_x given by McHardy and by Jones and Forman, for clusters listed in both of these papers,

shows the UHURU luminosities larger than Ariel-5 luminosities by .123

dex for R=2, by .105 dex for R=1, but by .278 dex for R=0 clusters.

In our own sample, we see no significant increase in EI or $\bar{T}$ with rich-

ness, but our sample is less than half as large as the samples in the

above two papers. If we plot $\bar{T}$ against the logarithm of the galaxy

counts represented by richness class for our sample (Figure 6) the

points are scattered in a roughly circular region around the concentration

at R=2 and $\bar{T} \approx 6$ keV, which appear to be average parameters for presently

observed X-ray clusters. There is no trend in R vs. $\bar{T}$ such as the

trend in $\bar{N}_0$ vs. $\bar{T}$ shown in Paper I; the clusters which ruin the pos-

sibility of such a trend are A1367, A2199, A2319, A2589, and A1254(?).

In Figure 7 we show the $\bar{N}_0$ vs. $\bar{T}$ correlation restricted to R=2 clusters.

The correlation persists, showing that $\bar{N}_0$ and $\bar{T}$ are correlated inde-

pendent of richness. The same result can be seen in the $\bar{N}_0$ vs. EI

correlation among R=2 clusters. Moreover, if the richness class 0,

1 and 3 clusters are added to the restricted correlations, in general

they fall among the R=2 clusters. McHardy (1977) also finds a BM type

vs. X-ray luminosity correlation which persists when restricted to

R=2 clusters. However, the converse does not seem to hold: Among

our cD and B type clusters, no richness dependence of $\bar{T}$ or EI is noticeable.

The same lack of a richness effect can be seen in Bahcall (1977).

We are forced to conclude from a critical appraisal of all the available

data that central cluster properties such as $\bar{N}_0$ and RS type are more

fundamentally correlated with X-ray luminosity (proportional to $\bar{T}^{-\frac{1}{2}}$

EI) than richness is.

Jones and Forman (1978) have argued that any correlations between morphology and X-ray luminosity are "artifacts" of a more fundamental richness-luminosity correlation or are selection effects. We have shown in Paper I that RS type is better correlated with EI than R. We have just concluded that $\overline{N}_0$ (which is related to RS type) is more fundamental than R. Therefore a better view might be that the richness-luminosity correlation seen by McHardy and, to a lesser extent, by Jones and Forman is dependent upon a more fundamental $\overline{N}_0$-luminosity correlation. The argument of Jones and Forman in support of their view boils down to a comparison of luminosity upper limits on cD and B clusters to those on R=2 clusters, among those clusters of potentially low luminosity because of insufficient observation. It is true that their upper limits on the latter are about twice those on the former. Yet we do not feel that this situation very strongly favors that existence of low-luminosity cD and B clusters over the existence of low-luminosity R=2 (or richer) clusters. The occurrence of low $\overline{T}$, R=2 clusters and low $\overline{N}_0$, R=2 clusters combined with our $\overline{N}_0$ vs. $\overline{T}$ correlation indicate that there is more than just a richness-luminosity correlation. Perhaps both $\overline{N}_0$ and R are significant parameters in determining the luminosity, but in different ways.

Therefore, it behooves us to consider the cases mentioned above, with multiple factors or time-varying X-ray properties. One such case is that in which central galaxy density, velocity dispersion, and perhaps morphology (which reflect the depth and steepness of the gravitational potential) determine the temperature, while $\overline{N}_0$ and to some extent richness determine the emission integral through a correlation with the

total mass of gas. Unfortunately, we have been unable to discover a numerical formula involving both $\bar{N}_0$ and R which predicts the EI values of our clusters more accurately than the simple power law fitted to the $\bar{N}_0$ vs. EI correlation, EI $\approx$ 4 x 10^{67} $(\bar{N}_0/20)^3$ cm^{-3}. If such a dual-parameter formula does not exist, we might look for evidence of time-varying cluster properties. Courie and Perrenod (1978) and Perrenod (1978a) have studied the time dependent response of gas to cluster gravitational potentials, and they find that cluster atmospheres approach structures similar to static solutions fairly quickly and retain these structures without large fluctuations after z $\approx$ .1 (which is the farthest distance to which we see X-ray clusters). However, evolutionary effects have been observed or deduced in optical cluster observations (e.g. Oemler 1974) and it seems possible that circumstances under which individual clusters form could be different enough to allow parameters such as EI to vary by factors of two or three at the present epoch, in clusters which will eventually be closer in EI. It is also possible, of course, that some of this scatter which worries us is just observational error, and we cannot reject that hypothesis until the optical and X-ray observations are refined.

VI. PREDICTIONS FROM CORRELATIONS

We have not yet used our correlations to make predictions. The scatter evident in all of them is a limitation to their utility, and all such predictions will have intrinsic uncertainties. Nevertheless some correlations are so significant that we cannot resist using the best fits at face value.

First we convert the known velocity dispersions of clusters into a histogram of predicted temperatures using the Δv vs. $\bar{T}$ relation (Figure 8a). A peak in the distribution of $\bar{T}$ appears at the surprisingly low temperature of 1 to 3 keV, rather than at the average $\bar{T}$ of clusters observed to date (Figure 8c) which is about 6 or 7 keV. We do not know what selection effects have prompted optical astronomers to measure the velocity dispersions of certain clusters, but at least the number of known Δv's is substantial. From a comparison of Figures 8a and 8c we predict a population of low temperature clusters, which should be of lower luminosity, of lower flux, and harder to observe than hotter clusters due to absorption. However, many of these low-velocity-dispersion clusters are nearby and should be discovered by HEAO-1 or HEAO-B.

One can also convert the $\bar{N}_0$ list of Bahcall (1977) into a similar histogram of predicted temperatures from the $\bar{N}_0$ vs. $\bar{T}$ relation (Figure 8b). This list was compiled from a 2 to 10 keV survey, however, and thus the predicted histogram is peaked near the peak of observed temperatures, 6 or 7 keV, and no clusters below 2 keV are seen. The absence of clusters with $\bar{N}_0$ predicting $\bar{T} > 10$ keV is curious and may imply some difference between $\bar{N}_0$ and Δv as measures of the gravitational potential for the most massive known X-ray clusters. Figure 8c seems to resemble Figure 8b in its peak and Figure 8a in its breadth. However, the two clusters with the highest $\bar{T}$ in our sample, Abell 1254 and 2142, fall outside either prediction of cluster $\bar{T}$ distributions. In Figure 8c we show a Gaussian fit, not including A2142, which has a mean of $\bar{T} \approx 7.0$ keV and a dispersion $\sigma \approx 3.8$ keV. With respect to this fit, Abell 1254

is 3σ from the mean and Abell 2142 is greater than 8σ from the mean. The isolation of these sources in the temperative histogram may be enough to conclude they are not the same type of cluster source as the others, perhaps being active galaxies within clusters.

A prediction of our EI vs. $\bar{T}$ correlation is that if there are true cluster X-ray sources more massive than any so far observed, their EI's will be extremely high, since luminosity rises so steeply with temperature. Extrapolation of this relation to the low temperatures just predicted above leads to the conclusion that such low luminosity objects will be very difficult to find.

Finally, all our correlations together imply that the observed X-ray core radius, obtained from fitting spatial profiles with isothermal spheres, is not related to the actual temperature of the gas within that radius but is rather some cutoff radius in the surface brightness distribution. The reasoning behind this is discussed further in the next section. The prediction from it is that observations with better resolution than those to date will show a surface brightness distribution within the overall profile which implies a core radius smaller than the core radius of the galaxies. This prediction apparently does not apply to Coma or Abell 2319A.

VII. IMPACT ON MODELS

What sort of generalized picture of an intracluster atmosphere is projected by our discussion thus far? The most important aspects are: 1) the correlation with depth of the gravitational potential; 2) the low value of γ_{eff} or the high value of ε; 3) the prevalence

of iron; 4) the temperature dependence of μ, R_x, and/or f. From these, one visualizes gas coming out of galaxies, falling toward the cluster center along with some primordial gas, and building up into a structure which is nearly isothermal in its higher temperature regions. Some of these points have been made in Paper I, and we refer the reader to the final section of that paper.

Interpretation of the low values of γ_{eff} requires more discussion. Since $\gamma = 5/3$ represents an adiabatic equation of state and $\gamma = 1$ an isothermal one, we must ask what physical process enforces near isothermality. Two possibilities are thermal conduction and central thermal instability.

Mathews (1978) has made a realistic estimate of thermal conduction rates in intracluster atmospheres. The rates depend on the correlation length of the intergalactic magnetic field, but if this length is assumed to be on the order of the diameter of the galaxies which stir it up, the rate is sufficient to enforce isothermality within a few core radii of the cluster center. Since conduction across a field is negligible, the magnitude of the field is irrelevant and only its geometry is of interest. Observations of radio tail sources (e.g. Rudnick and Owen 1977) probably show that the movement of a galaxy through the gas causes the field to string out behind the galaxy. Turbulence within the tail (Pacholczyk and Scott 1976) should have some effect on the correlation length long after the galaxy has passed, but whether it should make this length much less than 10 kpc is difficult to determine. One process which may bear upon the large scale field geometry is the "orbit segregation" recently suggested by Saslaw (1977). He finds that predominantly

radial galaxy orbits accumulate in the center of a slowly contracting cluster while predominantly circular orbits spiral in more slowly, due to the different time averaged gravitational field sampled by the two types of orbits. If galaxies on the radial orbits pull the intergalactic field behind them, the field in the central parts of a cluster could also become predominantly radial, leading to an anisotropic correlation length. This is further reason to expect a value at least on the order of 10 kpc for the radial correlation length. However, observations of cluster radio haloes (e.g. Jaffe 1977) may imply that the magnetic correlation length is small, perhaps only $\sim$ 1 kpc.

The net rate or timescale for heat conduction over some distance also depends on the local gas density. Spatially resolved X-ray profiles of clusters prove that the density falls off quickly beyond a few core radii (cf. §IIb). It is thus likely that the conduction rate drops quickly at about the same radius, causing gas further out to be less coupled to the heat source at the cluster center generated by compression of the gas and causing the temperature to fall. This is equivalent to an increase in γ_{eff} beyond this radius. This fact could explain why the specific kinetic energy ratio ε is greater than 1, indicating that the gas is less extended than the galaxies under isothermal assumptions, while fits of isothermal spheres to observed spatial profiles of cluster sources seem to show the gas more extended than the galaxies. The radius beyond which conduction is unimportant helps determine the spatial profile observed in the kilovolt X-ray range, leading to a discrepancy between the actual X-ray core radius and the apparent X-ray core radius for

an infinite isothermal sphere. The density profiles in Perrenod's (1978a)

mass injection models also have cutoffs, but these models are not pertinent

for other reasons, as discussed below.

The alternate process capable of causing clusters to have γ_{eff}

close to one is central thermal instability, in which continual central

collapse causes a steady inflow of intracluster gas. Dissipation in

the central gas also provides a ready explanation of $\varepsilon > 1$, i.e. why

the gas has a lower remaining specific thermal energy than the specific

kinetic energy of the galaxies. Realistic models of this type have

been discussed by Cowie and Binney (1977), Mathews (1978), Cowie and

Perrenod (1978), and Mathews and Bregman (1978). In this case, we need

to inquire whether our evaluation of γ_{eff} from our synthetic polytropic

spectra is still valid for these nonhydrostatic models. Fortunately,

the gas flow in these models always has a rather low Mach number: This

implies directly that the advective kinetic energy density in the flow

is much less than the thermal energy density, so that we do not go far

wrong in using hydrostatic model spectra compared with data to deduce

the slope of the equation of state. Hence our conclusion that γ_{eff}

$\approx$ 1.1 should apply to subsonic dynamic models as well. If one plots

the pressure and density taken from Figure 1 of Cowie and Binney, the

logarithmic slope of this effective (radially dependent) equation of

state is very close to one for the range of densities found at 0.5 to

5 galaxy core radii from the center. Farther out, this equation of

state steepens, and at the center it flattens, as expected. This particular

model which they graph does not include thermal conduction, but others

in their paper do. It is not hard to understand why an inflow model, including radiative cooling, produces an isothermal effective equation of state without conduction: If gas falls from a radius r_1 to r_2 toward the cluster center but cools as it falls, then the gas will not gain the full adiabatic pressure increment due to the geometric compression factor $(r_1/r_2)^2$. Instead, since the temperature at r_2' is lower than the value it would have in an adiabatic flow, the structure of the gas can be approximated by a polytrope of index $\gamma_{eff} < 5/3$, as observed.

What is the evidence that helps us choose between thermal conduction models, cooling inflow models, or models including both conduction and cooling, as an explanation for the low values of γ_{eff}? On the one hand, timescales for radiative cooling are not short enough to be of interest unless central densities are over 10^{-3} cm^{-3}. It is doubtful whether densities ever rise that high in all of our clusters with low γ and high ϵ. Cowie and Perrenod have indicated that such gas structures can be established in realistic situations, but from more sophisticated models, Perrenod (1978) seems to reverse this conclusion. Also, the fit to the spatial profile of Coma in Cowie and Binney is barely acceptable, while polytropic models with a cutoff should provide better fits. However, soft X-ray maps of Perseus and Virgo seem to show smaller sizes than in the 2 to 10 keV band (Gorenstein et al. 1977), which may be consistent with some cooling at the center. Further spatial observations are necessary to resolve this point.[1] On the other hand, thermal conduction

---

[1] In any case, the cooling center would emit largely at lower energies

than 2 keV, while the larger region around it emits the 2 to 20 keV

X-rays observed by OSO-8. This region remains close to a hydrostatic

polytropic structure with cutoff, so that cooling inflow models have

little effect on the interpretation of the data in Paper I, unless accretion

onto a central massive galaxy produces a compact source of thermal or

nonthermal X-rays (but see Mathews and Bregman).

---

models require a correlation length for the magnetic field greater than

about 10 kpc in the radial direction. One cannot show that this require-

ment is satisfied or not satisfied. Models with both conduction and

cooling have been discussed by Cowie and Binney, by Cowie and Perrenod,

and by Perrenod, and should be considered as the most general models

for analysis.

The other point requiring more discussion is the interpretation

of the temperature dependence of EI. In §IV we decided that μ must

increase with cluster temperature. Since higher temperature seems to

be associated with a more massive core ($\overline{N}_0$ vs. $\overline{T}$, Δv_c vs. $\overline{T}$), perhaps

the natural end result of evolution of more massive clusters is higher

gas densities. Then stripping of interstellar gas into the intergalactic

medium would be more efficient in hotter clusters, perhaps giving μ

the required temperature dependence. However, it is not clear from

present theoretical work that a steep enough $\mu(T)$ would result, and

our inability to factor $\mu^2 f/V$ with good confidence forces us to consider

other explanations. The key parameter in understanding the EI vs. $\overline{T}$

correlation is the specific mass injection rate per unit cluster mass,

including galactic and primordial mass injection, since this rate determines

how gas builds up around the cluster center. As an example of the complications possible, note that if a higher injection rate causes f to decrease, the effect of greater μ is diluted. To make this more clear, imagine the evolution of a cluster atmosphere which has already reached equilibrium at the center but still is accreting the gas continuing to be expelled from cluster galaxies: The central density cannot rise above the value it had when the central temperature first reached its equilibrium level, unless there is dissipation, and then the rate of dissipation determines how fast the density rises. To predict the density evolution beyond the core radius and to distinguish the effects of continued accretion on the 2 to 20 keV EI, it is clear that one needs detailed hydrodynamic models with appropriate local physics.

The territory of detailed hydrodynamic models is still being explored. Cowie and Perrenod (1978) and Perrenod (1978a) have considered mass injection models with conduction and cooling. Unfortunately they do not calculate f or $\overline{T}$ for their models, so it is impossible to use most of their results in our practical analysis. Although Perrenod tabulates the X-ray core radius and finds it to be larger than 0.25 Mpc for all mass injection models except one with saturated conduction, he calculates the core radius in the ½ to 2 keV band. The core radius in our band should be significantly smaller. The spectra to be expected from the nonconductive models of Perrenod may well be inappropriate for our clusters both because these spectra deviate from isothermal spectra and because the temperatures reached are too high for the Coma cluster, which he claims to be modeling. Additional evolutionary

calculations such as Perrenod's performed with an eye toward explaining our results, should be very rewarding. In particular, the isothermality of cluster spectra indicates that conduction models should be run with a variety of magnetic correlation lengths.

VIII. RELIABILITY OF THE IRON ABUNDANCE DETERMINATIONS

Since astronomers are likely to make free use of the result that intracluster gas contains about half the solar abundance of iron, it is well to consider the reliability of this result. This reliability is a separate question from experimental or statistical uncertainty, which can be estimated graphically from Figure 2 of Paper I. It is instead a question of uncertainty in the underlying chain of physical reasoning which links an experimentally determined equivalent width for the 6.7 to 7 keV iron line feature to an iron abundance. The chain begins with the assumptions that the iron line originates in the same gas as the X-ray continuum and that this gas is in a statistical equilibrium dominated by collisions. The first assumption is wrong if the iron line originates in galaxies, but this has been adequately discussed before (references in Paper I), or if intracluster atmospheres have abundance gradients (Fabian and Pringle 1977). The second assumption is wrong if the ionization state of the gas is not yet an equilibrium state (very unlikely considering the timescale involved for equilibration) or if photoionization by a photon field unrelated to the local electron temperature of the gas plays a role in determining ionization equilibrium[1]. If these

---

[1] In models such as polytropic models with large γ, the density falls off with increasing radius faster than the local X-ray flux from the

hot central region, until at some radius, often less than an Abell radius, the photoionization rate of elements like silicon is comparable to the collisional ionization rate. However, the contribution of photoionized gas at such low densities to the overall X-ray flux of a cluster is negligible, except perhaps in certain soft X-ray lines.

---

assumptions are accepted, the calculation of the iron abundance follows from a comparison of the observed line-to-continuum ratio to the ratio expected on the basis of a theoretical calculation of the line emission from a hot plasma. For purposes of the following discussion, we will call a calculation using atomic data as input and giving an X-ray spectrum as output a "spectrum calculation". Uncertainties in these theoretical calculations have heretofor been ignored in the literature on X-ray clusters, but they have a bearing on the reliability of iron abundance determinations.

Different experimental groups have derived different iron-to-hydrogen ratios from very similar iron line equivalent widths (EW). For example, Mitchell et al. (1976) have found Fe/H $\approx$ 3 x 10^{-5} by number from EW $\approx$ 360 eV for the Perseus cluster while we have found Fe/H $\approx$ 1.4 x 10^{-5} from EW $\approx$ 400 eV. The difference is not due simply to different measured continuum temperature, but implies a different interpretation of the results of atomic physics available in the literature. Since references to atomic physics literature are given in the X-ray cluster papers, one could in principle discover the exact reason for any discrepancy among the scores of individual cross sections used in spectrum

calculations. This turns out to be impratical unless each group is willing to make the effort to lay all their computer cards on the table. It is hoped that this will be done soon, since in some cases the accuracy of the data has surpassed that of the computations. To begin with, we will bypass the uncertainties in spectrum calculations relating to exactly how the atomic physics is used and which processes are included, and consider instead the ranges of results within the atomic physics itself.

While line energies assigned to different atomic transitions in solar X-ray spectra are probably dependable for astrophysical use, excitation cross sections and similar results cannot often be reliably computed from solar spectra, because the physical conditions in the line formation region on the sun are not well known. An important limitation is that density clues are rare and even when found are strictly useful only for lines of the one ion employed. In the work used in Paper I to derive iron abundances, namely the spectrum calculation of Raymond and Smith (1977), use of such solar observational cross sections has been almost eliminated for lines contributing to the 6.7 to 7 keV iron line blend. In particular, the most important data, collisional excitation cross sections for helium-like ions, have been taken from theoretical computation rather than solar observations.

Of course, the theoretical computations of cross sections have some range of confidence themselves. Distorted wave approximations have been used by a variety of workers, including Jones (1974) and Davis, Kepple, and Blaha (1977) and have a potential accuracy of a few percent. Since the claimed accuracy of the best calculations is 10 to 20 percent

and there is the possibility of unincluded channels, we favor a pessimistic estimate of uncertainties in such cross sections, roughly 30%. This estimate applies to direct collisional excitation of helium-like transitions, and most other relevant cross sections have larger errors. Since the spectrum calculations which use the cross sections also depend on an ionization equilibrium calculation, the net uncertainty in EW will be somewhat larger, probably 50 to 75%, in the temperature range where direct collisional excitation is the dominant process contributing to the iron line blend. For the cluster iron lines, this range is 3 keV $\lesssim$ T $\lesssim$ 30 keV.

However, line emission for T $\lesssim$ 3 keV is dominated by satellite transitions. Available calculations of the strengths of these satellites have greater probable errors than those for lines in helium-like ions. Again, comparison of spectrum calculations ostensibly using similar atomic input data shows discrepancies symptomatic of the problems; the EW vs. T curve given in Figure 2 of Paper I (a representation of the results of Raymond and Smith), that given by Bahcall and Sarazin (1978), and that estimated by Malina et al. (1978) are similar in shape but differ at low temperatures. Until these discrepancies are understood, we are left with large uncertainties in iron abundances, a factor of 2 or more, for lower temperature clusters, for instance Virgo and Abell 1367. To make matters worse, attention has been drawn to a new process by Jacobs et al. (1977a,b) which has not been included, to our knowledge, in any comprehensive spectrum calculation. This process, autoionization leaving an ion in an excited state, impacts the EW vs. T curve at low temperatures in several ways. The changes that must be made in the

EW vs. T curve are difficult to predict.

Finally, it is well to point out that a 10% helium abundance increases bremsstrahlung emission by more than 40% over that of a pure hydrogen gas, since this emission is proportional to the square of the ion charge and since the free-free gaunt factor turns out to be larger for helium nuclei than for protons at the same temperature in the keV range. Therefore, the choice of helium abundance affects the iron abundance derived from the equivalent width. Paper I used He/H - 8.5% by number. The change in derived iron abundance due to a change in helium abundance from 8% to 10% is almost 10%. Of course, the helium abundance in intergalactic gas in distant clusters is unknown. The inclusion of bremsstrahlung emission due to ions of elements heavier than helium is overall a smaller effect.

In summary, iron abundances for thus far observed clusters of average temperature, including all those with $T \gtrsim 3$ keV, have a probable error due atomic physics uncertainty alone of at least 50%, while for $T \lesssim 3$ keV the error increases to at least 100%.

IX. CONCLUSIONS

We collect here the conclusions reached from this investigation. The first three depend on certain assumptions, which are therefore stated again here.

1) If intracluster gas is hydrostatic or at least has a rather low Mach number, and if the equation of state is restricted to polytropic forms, the logarithmic slope of the equation of state is about 1.1 in the 2 to 20 keV X-ray emitting regions of most clusters. This conclusion is not very dependent on the level to which gas fills the potential,

as long as $x_{out} \gtrsim 10$.

2) If intracluster gas is (nearly) isothermal in these regions, it has an X-ray core radius less than the core radius of the galaxies.

3) If the X-ray sizes of clusters measured by Kellogg and Murray (1974) and the X-ray temperatures of Paper I are interpreted as showing an increase in size with X-ray temperature, then hotter clusters have a larger fraction of their virial mass in the form of hot intracluster gas than cooler clusters do.

4) Bahcall's (1977) central galaxy density $\overline{N}_0$ correlates with X-ray properties of clusters better than richness or the galaxy density defined by van den Bergh and deRoux (1978). $\overline{N}_0$ is related to optical cluster morphology. Correlations of $\overline{N}_0$ and morphology with X-ray properties are not "artifacts" of indirect richness correlations.

5) The probable error in most cluster iron abundance determinations, such as those in Paper I, is about $\pm$ 50% from atomic physics uncertainties alone, if the cluster temperature is $\gtrsim$ 3 keV. If T $\lesssim$ 3 keV, the error increases to more than 100%.

6) We predict a population of low T, low L_x clusters that have not yet been observed.

7) The inner regions of intracluster atmospheres must have some kind of isothermalizing dissipation, either thermal conduction, radiative cooling, or both.

8) Therefore the best model for these atmospheres is one in which: a) mass is ejected from galaxies; b) it falls toward the cluster center; c) it approaches a quasisteady structure which is nearly isothermal

within some boundary radius at which a sharp density cutoff occurs; and d) therefore this cutoff should occur where the observed X-ray profiles drop off, while a more sharply peaked profile is entirely within the observed profile.

TABLE 1

VALUES OF THE SPECIFIC KINETIC ENERGY

RATIO ε

CLUSTER	Δv (km-s^{-1})	kT (keV)	ε	ε_c
A401	1390	6.7	1.81	2.48
A426	1396	6.8	1.79	2.45
A1060	771	3.1	1.20	1.64
A1367	847	2.8	1.60	2.19
Virgo	705	2.2	1.41	1.93
Centaurus	945	5.3	1.06	1.45
Coma	900	8.9	0.57	0.78
A2029	1151[*]	6.2	1.35	1.85
A2147	1120	7.2	1.09	1.49
A2199	843	3.2	1.39	1.90
A2256	1274	7.0	1.45	1.98
A2319A	873	12.5	0.38	0.52
A2319A,B	1627		1.33	1.82

---

[*]Average of the two values of Δv given by Faber and Dressler (1976).

TABLE 2

VALUES OF THE TEMPERATURE RATIO

$$\tau \equiv \overline{T}/T_c$$

kT_c(keV)	3			10			30		
x_{out}	10	40	100	10	40	100	10	40	100
γ									
1.05	1.00	1.00	1.00	1.00	1.00	1.00	1.00	1.00	1.00
1.10	1.00	.99	.99	1.00	.99	.99	.99	.99	.98
1.15	.99	.96	.95	.98	.95	.94	.97	.94	.93
1.20	.96	.92	.90	.94	.89	.87	.93	.87	.85
1.3	.89	.81	.78	.85	.75	.72	.79	.70	.66
4/3	.86	.78	.75	.81	.71	.68	.76	.64	.60
1.4	.82	.72	.69	.75	.64	.60	.69	.56	.50
1.5	.76	.65	.62	.68	.56	.50	.60	.46	.39
1.6	.72	.61	.57	.62	.50	.44	.53	.39	.32
5/3	.69	.59	.55	.60	.46	.41	.50	.35	.29

TABLE 3

POSSIBLE TEMPERATURE FUNCTIONS

	Case 1: μ independent of $\overline{T}$, $f \propto \overline{T}^{\delta}$	Case 2: f independent of $\overline{T}$, $\mu \propto \overline{T}^{\zeta}$
Case A: $R_X \propto \overline{T}^{\eta}$, $1.2 \lesssim \eta \lesssim 1.8$	$3.2 \lesssim \delta \lesssim 8.5$	$1.6 \lesssim \zeta \lesssim 4.3$
Case B: V independent of $\overline{T}$	$-0.4 \lesssim \delta \lesssim 3.1$	$-0.2 \lesssim \zeta \lesssim 1.6$

TABLE 4

AVERAGE INDICATORS OF GALAXY DENSITY

Quantity Averaged	Description of Sample	Number of Clusters in Sample	Average Value	Sample S.D.
$\bar{N}_0$ [*]	$R = 2$	14	26.6	6.9
$\bar{N}_0$	$k\bar{T} > 6$ keV	9	26.2	7.8
$\bar{N}_0$	$k\bar{T} < 6$ keV	5	15.2	3.3
$\bar{N}_0$	$<\rho>$[#] > 60	8	22.3	6.7
$\bar{N}_0$	$<\rho> \, < 60$	8	23.5	9.0
$\bar{N}_0$	$EI > 8 \times 10^{67}$	6	30.8	3.7
$\bar{N}_0$	RS type cD	12	25.9	8.0
$<\rho>$[#]	BM type I, $0.1 < z \leq 0.15$	18	39.8	29.6
$<\rho>$	BM type II, $0.1 < z \leq 0.15$	90	30.7	18.2

[*]All samples involving $\bar{N}_0$ were taken from list of Bahcall (1977). Units of $\bar{N}_0$ are galaxies per $\pi/4$ Mpc^2, estimated error is $\pm$ 20%.

[#]Values of $<\rho>$ were calculated using expression in van den Bergh and deRoux (1978) from data in Leir and van den Bergh (1977). Units of $<\rho>$ are galaxies per unit volume, normalized arbitrarily in the same way as in van den Bergh and deRoux.

REFERENCES

Abell, G. O. 1958, Ap. J. Suppl., 3, 211.

Bahcall, J. N., and Sarazin, C. L. 1978, Ap. J., 219, 781.

Bahcall, N.A. 1975, Ap. J., 198, 249.

Bahcall, N.A. 1977, Ap. J. (Letters), 217, L77.

Bautz, L. P., and Morgan, W. W. 1970, Ap. J. (Letters), 162, L149.

Cavaliere, A., and Fusco-Femiano, R. 1976, Astr. Ap., 49, 137.

Cooke, B. A. 1978, invited talk at meeting of A.P.S., Washington, D. C.

Cowie, L. L., and Binney, J. 1977, Ap. J., 215, 723.

Cowie, L. L., and Perrenod, S. C. 1978, Ap. J., 219, 354.

Davis, J., Kepple, P. C., and Blaha, M. 1976, J. Quant. Spectrosc. Rad.
    Transf., 16, 1043.

Faber, S. M., and Dressler, A. 1976, Ap. J. (Letters), 210, L65.

Fabian, A., and Pringle, J. 1977, M.N.R.A.S., 181, 5P.

Field, G. B., and Perrenod, S. C. 1977, Ap. J., 215, 717.

Gorenstein, P., Fabricant, D., Topka, K., Tucker, W., and Harnden, F. R.
    1977, Ap. J. (Letters), 216, L95.

Grindlay, J. E., Parsignault, D. R., Gursky, H., Brinkman, A. C., Heise,
    J., and Harris, D. E. 1977, Ap. J. (Letters), 214, L57.

Gunn, J. E., and Gott, J. R. 1972, Ap. J., 176, 1.

Jacobs, V. L., Davis, J., Kepple, P. C., and Blaha, M. 1977a,b, Ap. J.,
    211, 605; 215, 690.

Jaffe, W. J. 1977, Ap. J., 212, 1.

Jones, C., and Forman, W. 1978, Ap. J., in press.

Jones, M. 1974, M.N.R.A.S., 169, 211.

Kellogg, E., and Murray, S. 1974, Ap. J. (Letters), 193, L57.

King, I. R. 1972, Ap. J. (Letters), 174, L123.

Lea, S. M. 1975, Ap. Lett., 16, 141.

Lea, S. M. 1977, in Muller, E. A., ed. Highlights of Astron., 4
        (Dordrecht: Reidel).

Lea, S. M., and DeYoung, D. S. 1976, Ap. J., 210, 647.

Lea, S. M., and Holman, G. D. 1978, Ap. J., in press.

Leir, A. A., and van den Bergh, S. 1977, Ap. J. Suppl., 34, 381.

Malina, R. F., Lea, S. M., Lampton, M., and Bowyer, C. S. 1978, Ap. J.,
        219, 795.

Mathews, W. G. 1978, Ap. J., 219, 413.

Mathews, W. G., and Bregman, J. N. 1978, Lick Observatory Bulletin, No. 798.

McHardy, I. 1978, preprint.

Mitchell, R. J., Ives, J. C., and Culhane, J. L. 1977, M.N.R.A.S., 181,
        25.

Mushotzky, R. F., Serlemitsos, P. J., Smith, B. W., Boldt, E. A., and
        Holt, S. S. 1978, Ap. J., in press (Paper I).

Oemler, A. 1974, Ap. J., 194, 1.

Pacholczyk, A. G., and Scott, J. S. 1976, Ap. J., 203, 313.

Perrenod, S. C. 1978a,b, submitted to Ap. J.

Raymond, J. C., and Smith, B. W. 1977, Ap. J. Suppl., 35, 419.

Rood, H. B., and Sastry, G. N. 1971, P.A.S.P., 83, 313.

Rudnick, L., and Owen, F. N. 1976, Ap. J. (Letters), 203, L107.

Saslaw, W. L. 1977, Ap. J., 216, 690.

Smith, B. W., Serlemitsos, P. J., Mushotzky, R. F., Boldt, E. A., and
        Holt, S. S. 1978, in preparation.

van den Bergh, S., and deRoux, J. 1978, Ap. J., 219, 352.

Willson, M.A.G. 1970, M.N.R.A.S., 151, 1.

Yahil, A., and Vidal, N. V. 1977, Ap. J., 214, 347.

FIGURE CAPTIONS

Figure 1   -   The central velocity dispersion is plotted against the observed best fit single temperature $\bar{T}$. The data points and their errors are repeated from Figure 5 of Paper I and can be identified from that Figure. The solid sloping lines show the loci of Δv_c and $\bar{T}$ for polytropic models, and the lines are labeled with values of γ, which is constant along each line while the central temperature T_c of the models varies. The curved dashed lines show the loci when T_c is constant while γ varies. Both sets of lines were calculated with $x_{out} = 40$.

Figure 2   -   The mean velocity dispersion and the central galaxy density (Bahcall 1977) are plotted for all clusters for which both quantities have been measured, in order to calibrate $\bar{N}_0$ statistically as an indicator of core mass. The two sloping lines cover the approximate range of acceptable normalizations for a fit assuming $\bar{N}_0 \propto \Delta v^2$. Velocity dispersions are from Faber and Dressler (1976) and Yahil and Vidal (1976). Where there is unusual controversy over the correct value of Δv, as for Abell 262 and 2255, two values are plotted with the preferred value having a solid error line. Abell 2029 is plotted using the average of the two values of Δv in Faber and Dressler. The typical error in $\bar{N}_0$ quoted by Bahcall is shown in the lower right corner.

Figure 3   -   The X-ray temperature $\bar{T}$ from Paper I vs. the X-ray core radius given by Kellogg and Murray (1974). Errors in $\bar{T}$ are

90% confidence except for Abell 262 which is 68% confidence
and thus plotted with a dashed error line. The sloping dashed line
is determined by the Virgo, Centaurus, Perseus, and Coma
points (see text), while the solid line show the flattest
slope consistent with all the data points weighted by their
errors. Neither line violates any of the upper limits.

Figure 4 - The central concentration factor f defined in the text is
shown in the upper graph as a function of the outer radius
x_{out} for several values of γ and x_{band}. Values of f have
been found by integrating the density distributions of poly-
tropic models out to x_{band}. The lower curve shows the
temperature at x_{band} in units of the central temperature T_c for
several values of x_{band}. The temperature profile in polytropic
hydrostatic models is independent of γ but depends on x_{out}.

Figure 5 - The $\overline{N}_0$ list of Bahcall (1977) plotted against Abell richness
class R, with each point labeled by its Rood-Sastry morphological
type. There is a correlation between $\overline{N}_0$ and R at about the
same level of confidence as between $\overline{N}_0$ and RS type. The
scatter in the two correlations is also about equal.

Figure 6 - Abell richness class R vs. observed X-ray temperature $\overline{T}$. The
right hand scale gives the galaxy counts used by Abell (1958)
to define his richness classes. Thus the dashed lines determine
the probable error limits to his galaxy counts, and within the
dashed boundaries points are plotted at arbitrary levels in
the vertical direction, their positions chosen to eliminate overlap

in 90% confidence error bars on $\overline{T}$ for different clusters. There does not appear to be any correlation between R and $\overline{T}$, from which we conclude that richness is not a very good measure of core mass.

Figure 7 - The $\overline{N}_0$ vs. $\overline{T}$ correlation, shown in Figure 7 of Paper I, when only clusters of richness class 2 are plotted. The correlation is present at about the same confidence as it is among clusters of all richness classes.

Figure 8 - Histograms of X-ray temperatures: a) predicted from optical velocity dispersion lists; b) predicted from Bahcall's (1977) $\overline{N}_0$ list; and c) best fits from Paper I observations by OSO-8. Each temperature $\overline{T}$ is binned in the 1 keV interval determined by its integer part. In a) and b), if $\overline{T}$ has been measured for a cluster and <u>disagrees</u> with that predicted, the observed $\overline{T}$ is binned in a solid numbered box and the predicted $\overline{T}$ is binned in a dashed box containing the same number. The clusters having such discrepancies are: 1) Perseus, 2) A1367, 3) Virgo, 4) Coma, 5) A2029, 6) A2147, 7) A2256, 8) A2319A, 9) A2199, 10) A2589, 11) Centaurus, and 12) SC1251-28. In c) a gaussian fit to the observed $\overline{T}$ distribution is superimposed. This fit takes into account all clusters except A2142, which was binned as ">20".
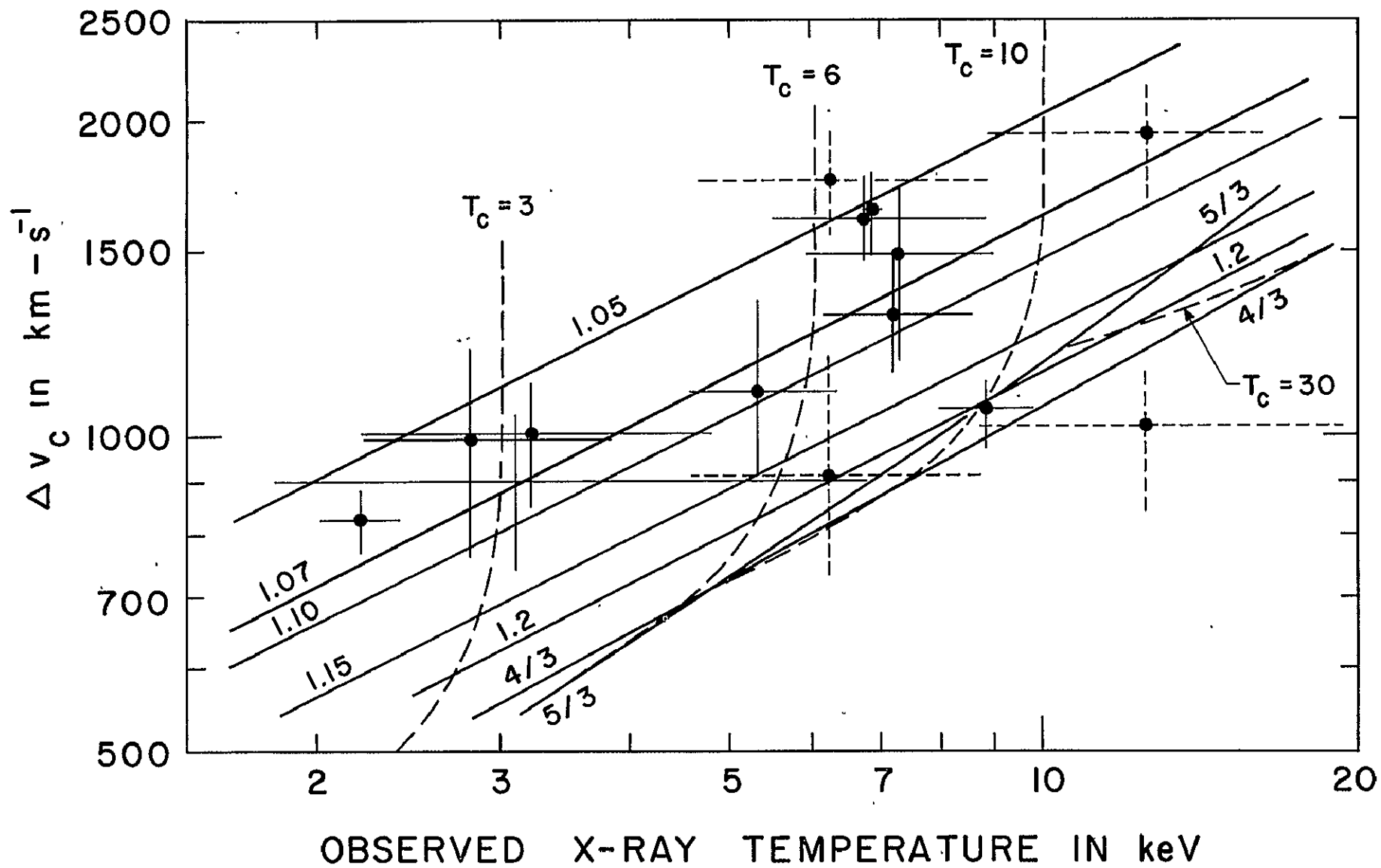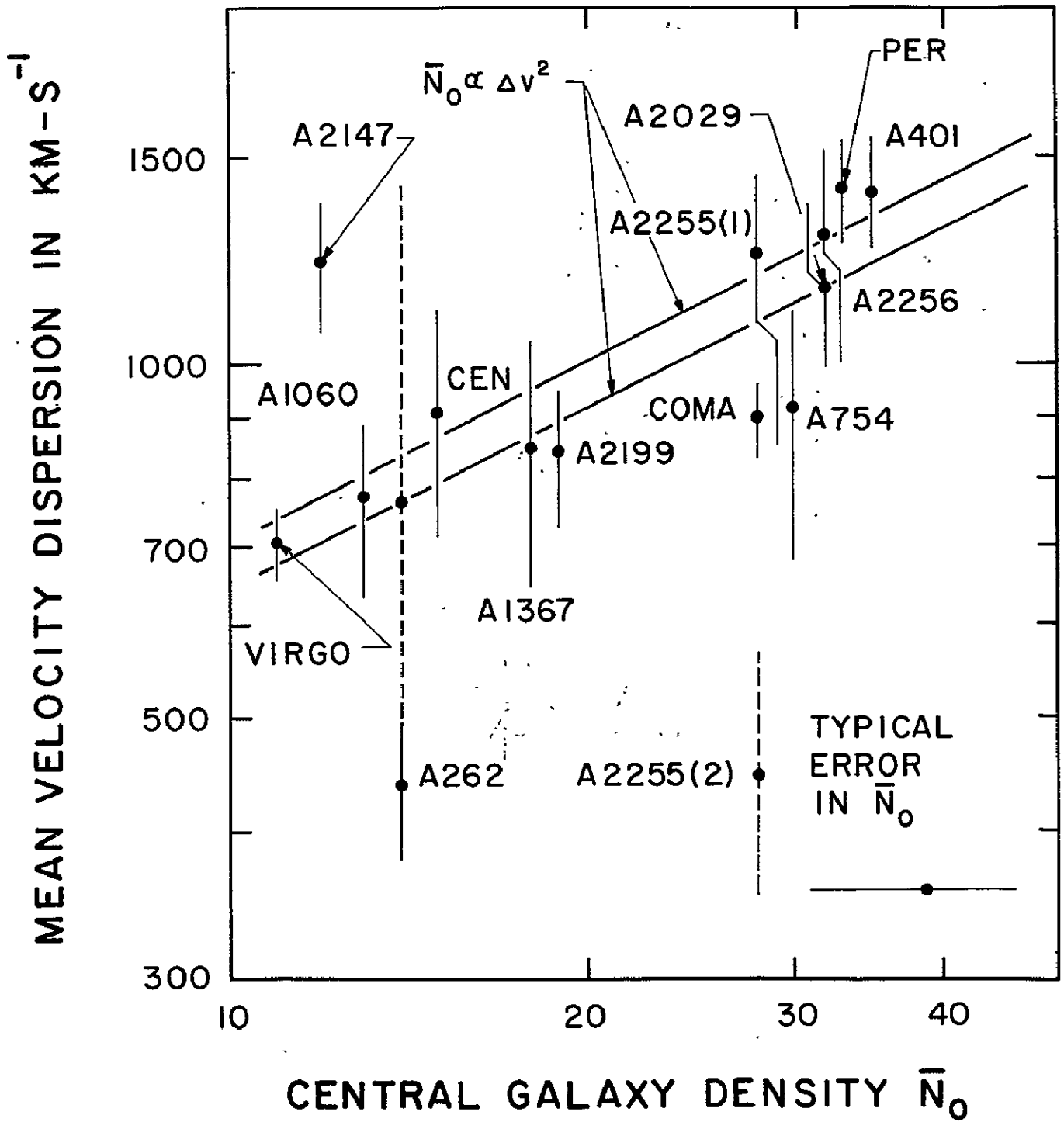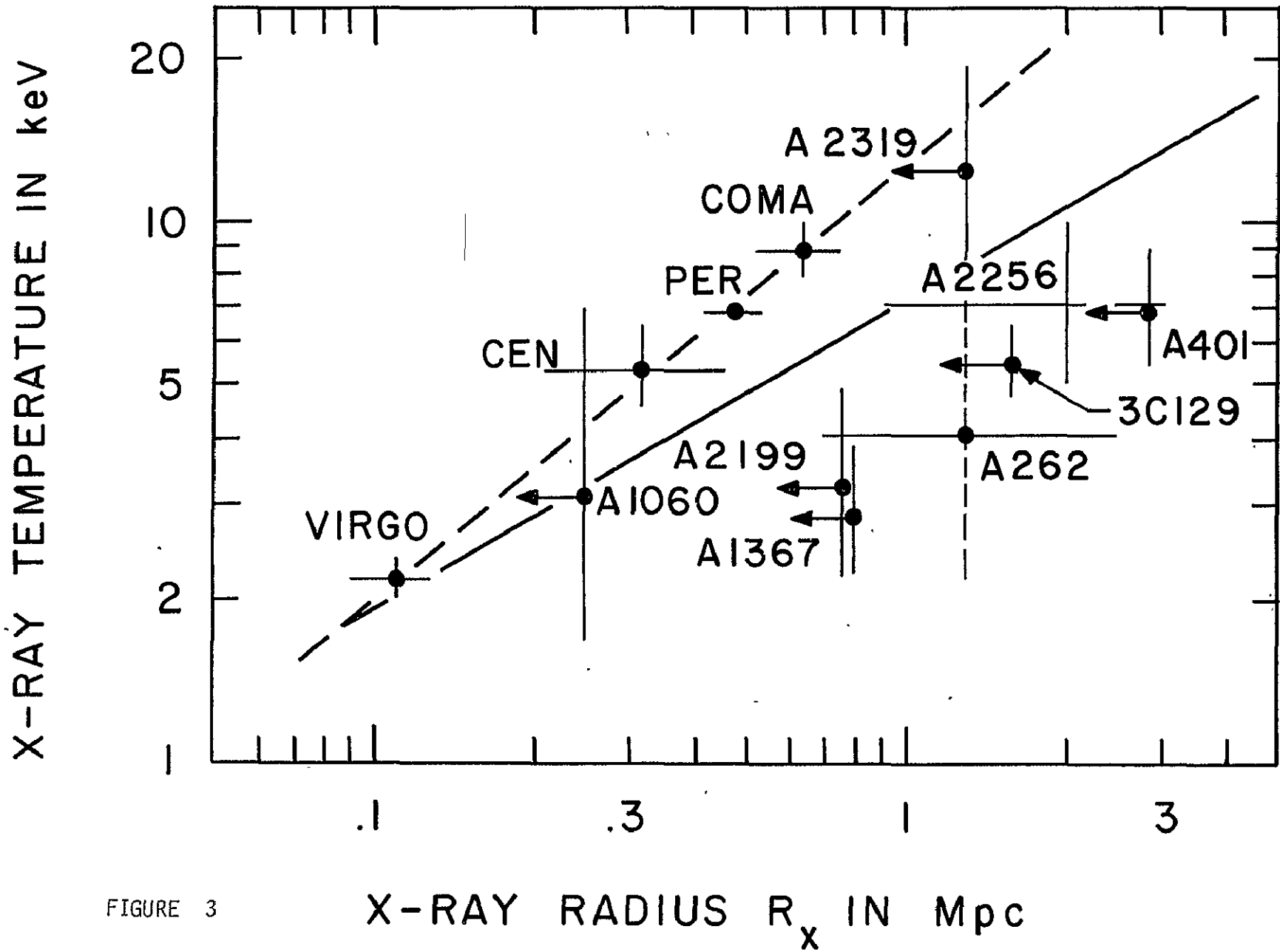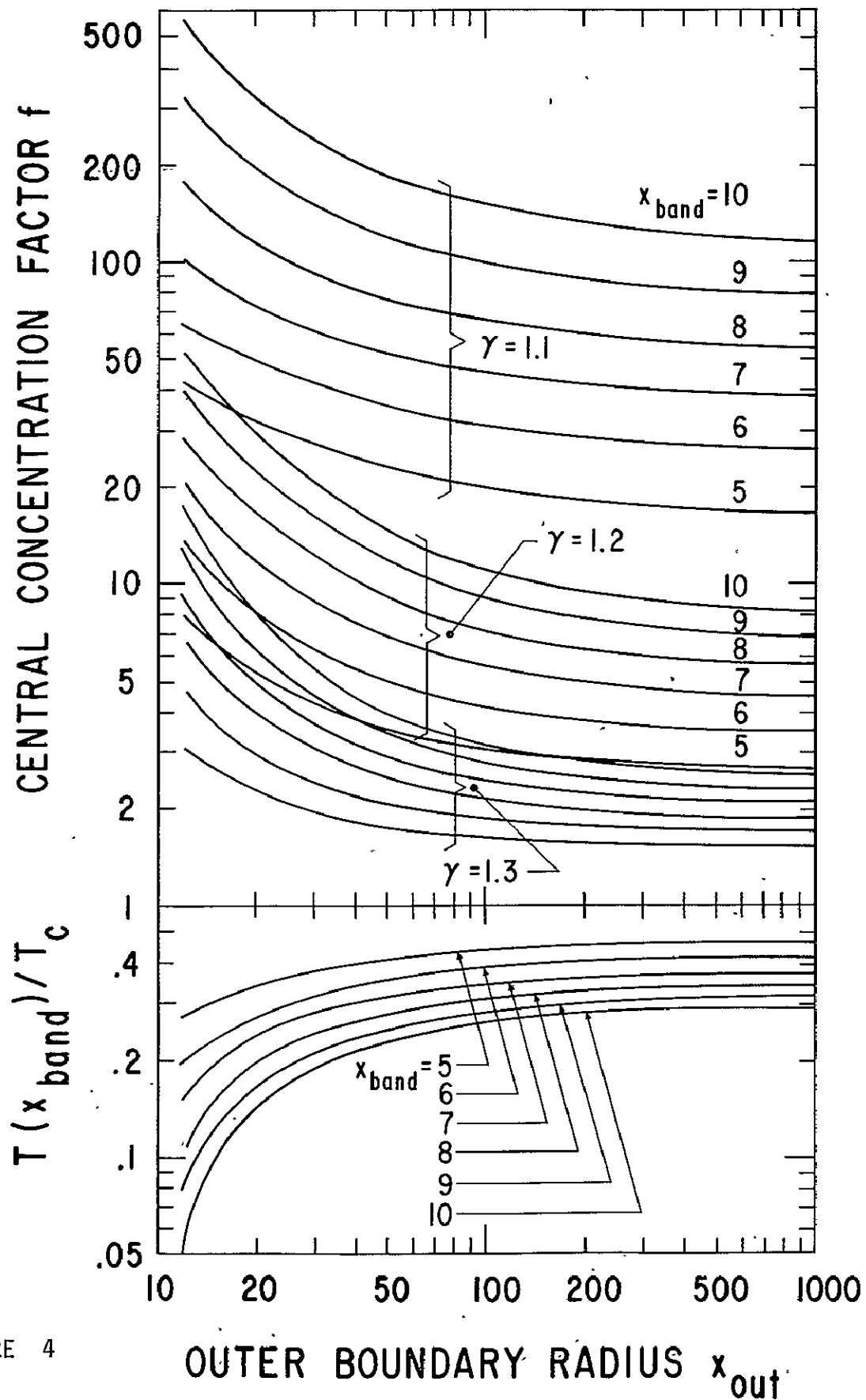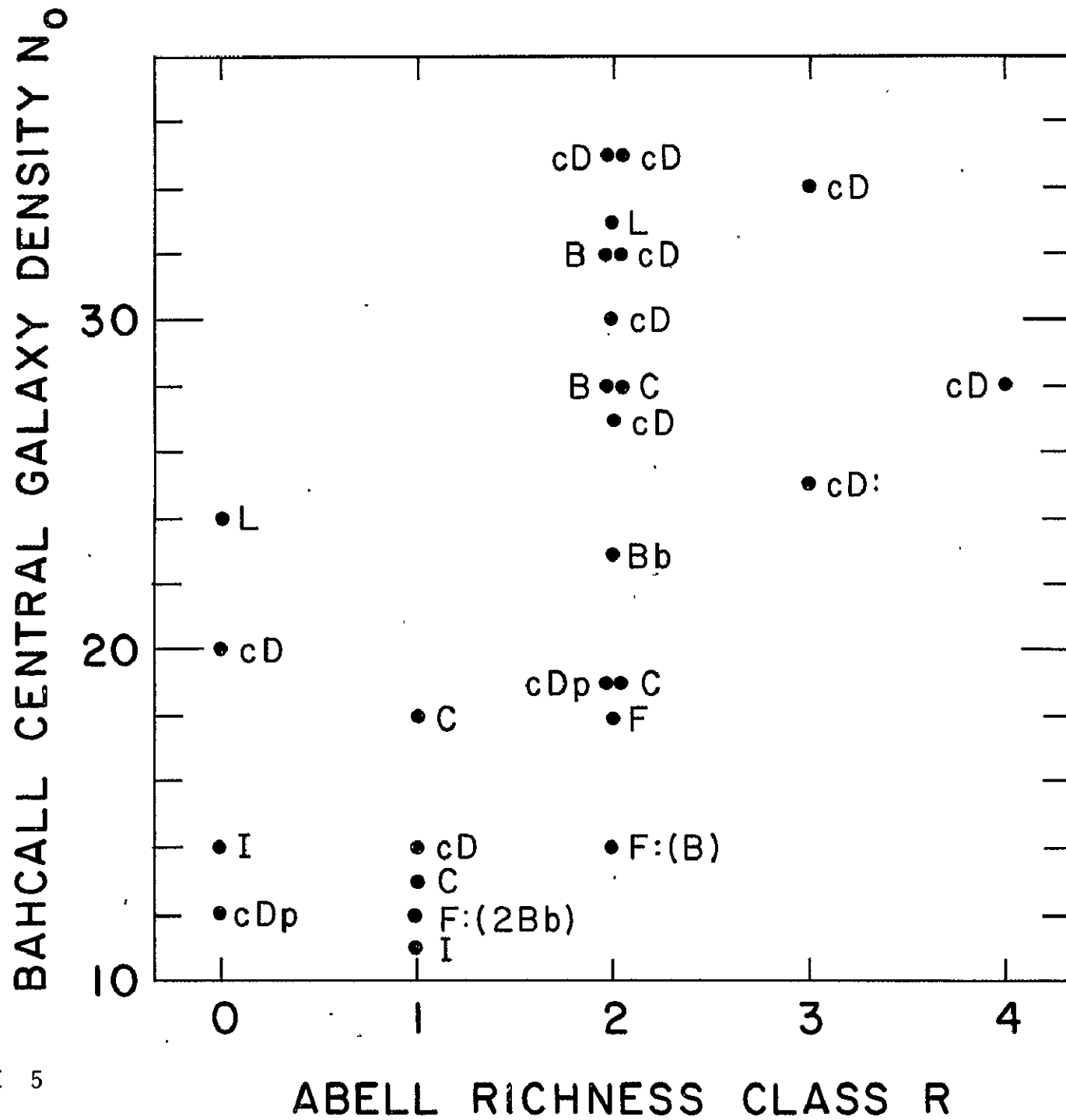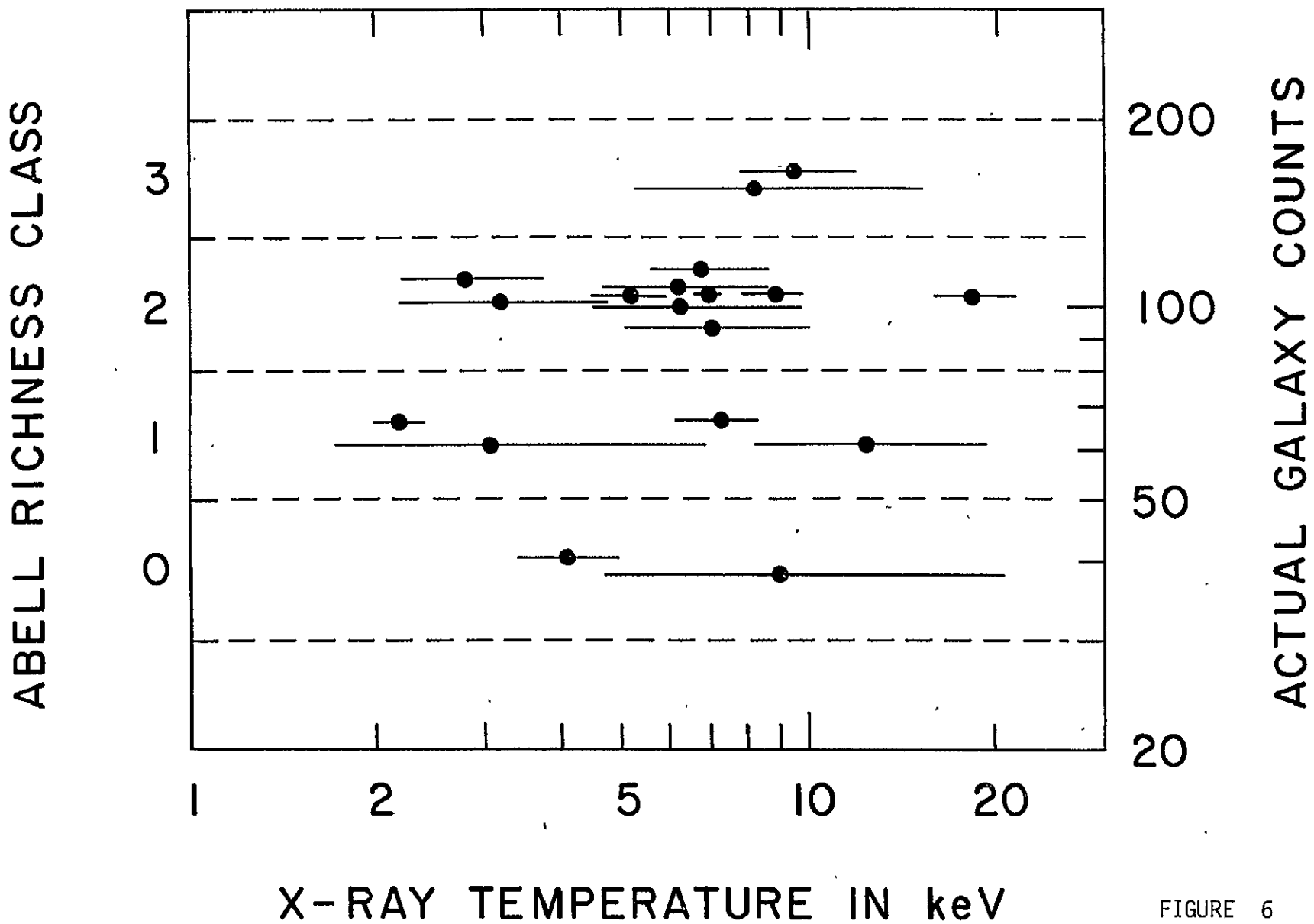
FIGURE 1

FIGURE 2

FIGURE 3

FIGURE 4

FIGURE 5

FIGURE 6

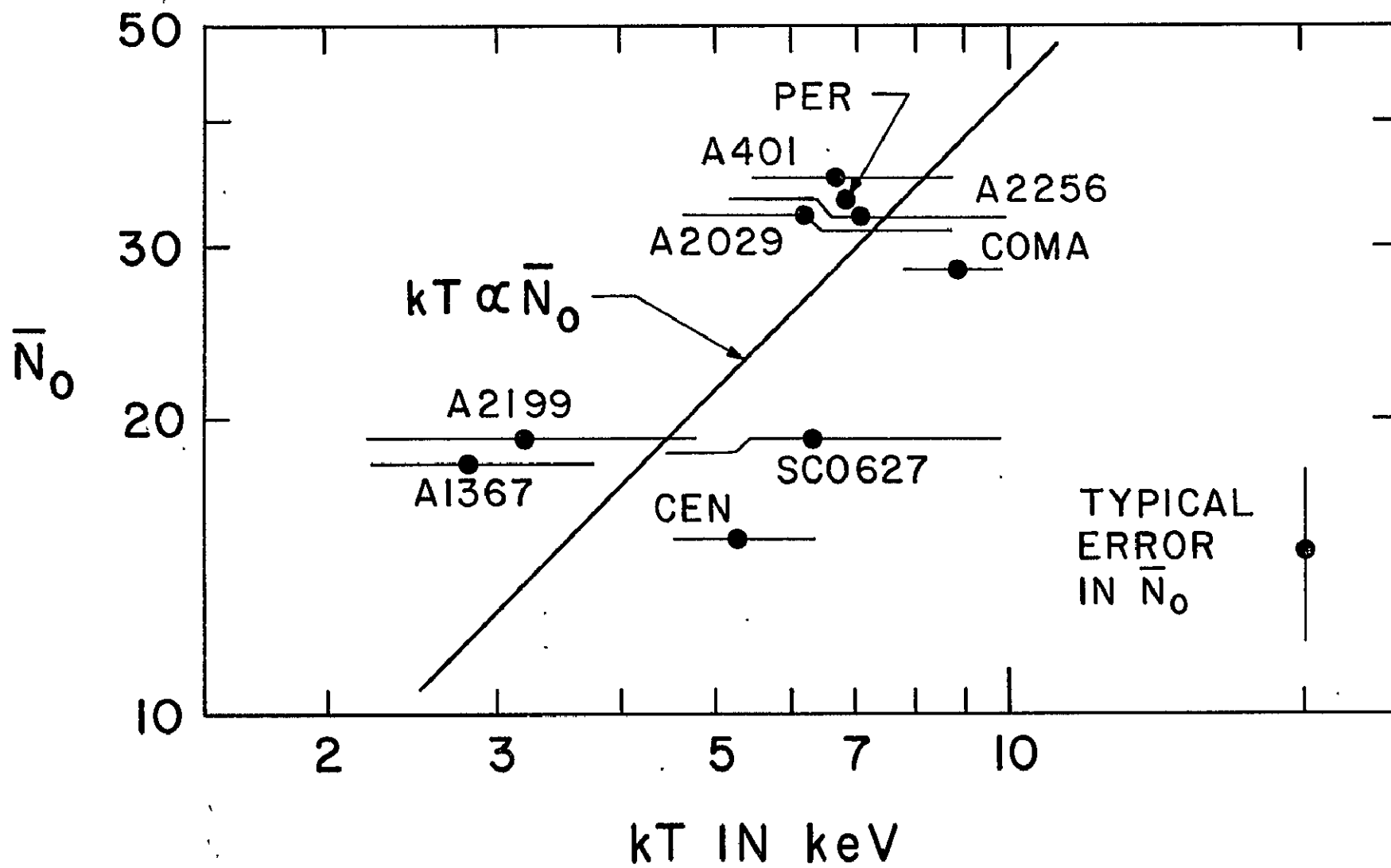FIGURE 7
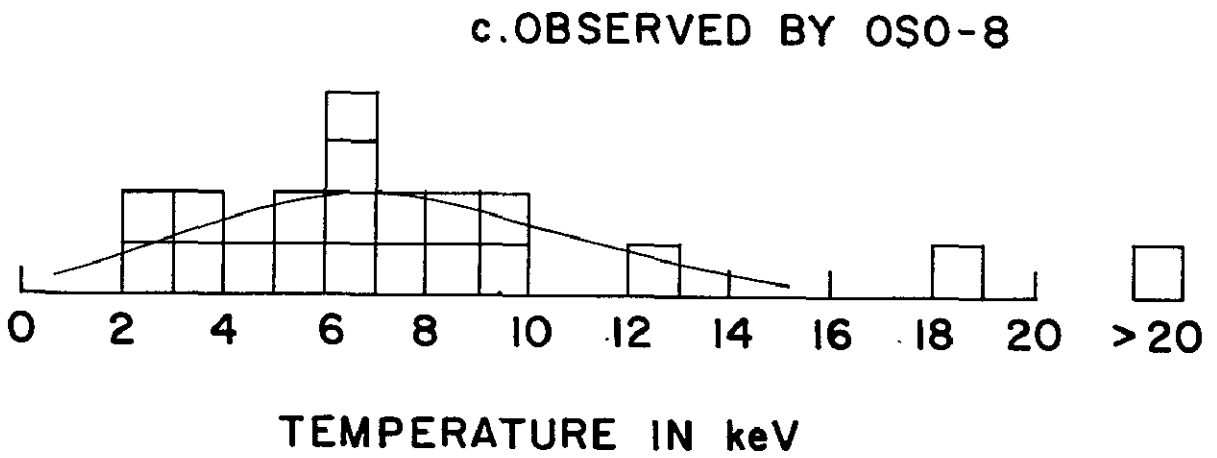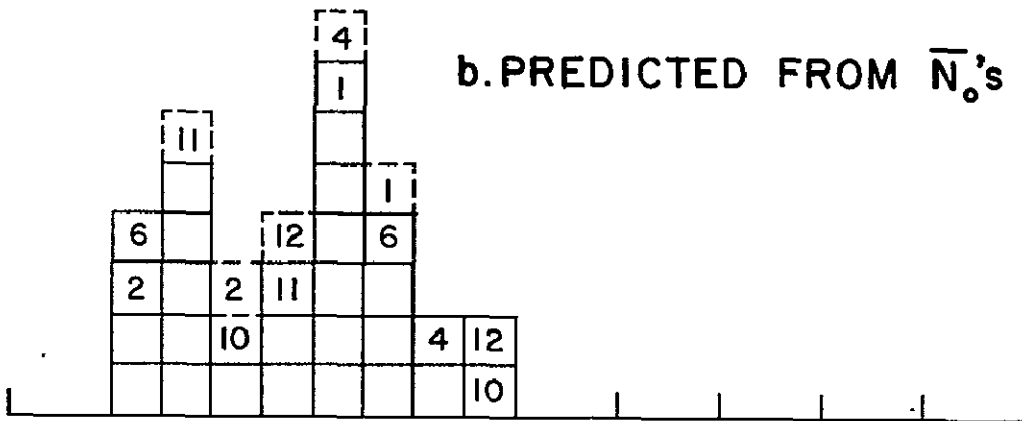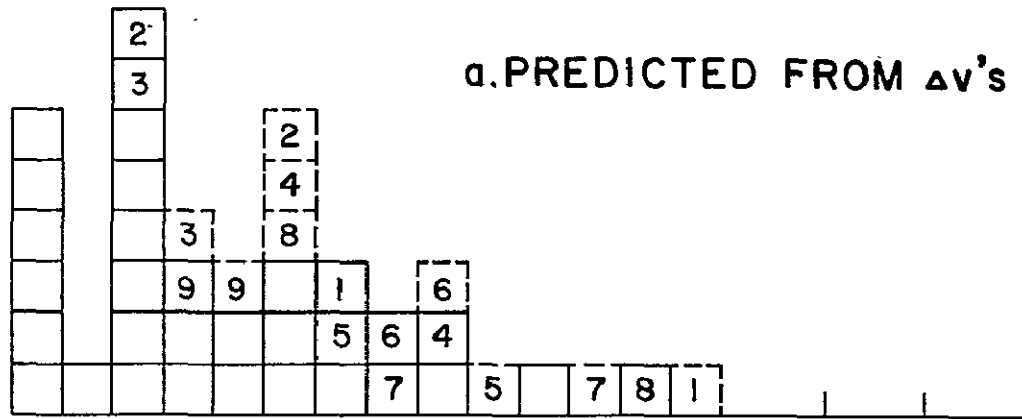
FIGURE 8

BIBLIOGRAPHIC DATA SHEET

1. Report No. TM 79577	2. Government Accession No.	3. Recipient's Catalog No.
4. Title and Subtitle OSO-8 X-RAY SPECTRA OF CLUSTERS OF GALAXIES. II. DISCUSSION		5. Report Date July
		6. Performing Organization Code 661
7. Author(s) Barham W. Smith (NAS/NRC), R.F. Mushotzky (U. MD), and P.J. Serlemitsos		8. Performing Organization Report No.
9. Performing Organization Name and Address Code 661 Cosmic Radiations Branch Laboratory for High Energy Astrophysics		10. Work Unit No.
		11. Contract or Grant No.
12. Sponsoring Agency Name and Address		13. Type of Report and Period Covered
		14. Sponsoring Agency Code

15. Supplementary Notes

16. Abstract

The Goddard Space Flight Center 2 to 20 keV OSO-8 data on X-ray clusters is examined for information which will restrict models for hot intracluster gas structures. Our starting point is the correlations between X-ray spectral parameters and optical cluster properties which we presented in a previous paper (Mushotzky et al.; Paper I).

From the correlation between X-ray temperature and velocity dispersion, we conclude that the X-ray core radius should be less than the galaxy core radius, if we assume the gas is isothermal. Thus fits of X-ray profiles of clusters to isothermal spheres yield a core radius approximately equal to the density cutoff radius rather than the true core radius. If we instead assume a generalized polytropic structure, from the same correlation one may conclude that the gas is more nearly isothermal than adiabatic within a few core radii of the center. Therefore we require thermal conduction, radiative cooling, or both in cluster atmospheres. In both of these interpretations, the Coma cluster and possibly Abell 2319A are quite discrepant.

From the correlation between bremsstrahlung emission integral and temperature, we conclude that hotter clusters contain a larger fraction of their virial mass in the form of gas emitting in the 2 to 20 keV band.

17. Key Words (Selected by Author(s))		18. Distribution Statement	
19. Security Classif. (of this report) U	20. Security Classif. (of this page) U	21. No. of Pages 58	22. Price*

GSFC 25-44 (10/77)